Master's Thesis

Atmospheric dependence on efficiency of perovskite solar cells fabricated with Zn_2SnO_4 electrode

Minjae Paik

Department of Energy Engineering

(Energy Engineering)

Graduate School of UNIST

2018

Atmospheric dependence on efficiency of perovskite solar cells fabricated with Zn_2SnO_4 electrode

Minjae Paik

Department of Energy Engineering
(Energy Engineering)

Graduate School of UNIST

Atmospheric dependence on efficiency of perovskite solar cells fabricated with Zn_2SnO_4 electrode

A thesis/dissertation
submitted to the Graduate School of UNIST
in partial fulfillment of the
requirements for the degree of
Master of Science

Minjae Paik

07. 09. 2018
Approved by

_____

Advisor
Sang Il Seok

Atmospheric dependence on efficiency of perovskite solar cells fabricated with Zn_2SnO_4 electrode

Minjae Paik

This certifies that the thesis of Minjae Paik is approved.

07/09/2018

signature

_____

Advisor: Sang Il Seok

signature

_____

Jin Young Kim

signature

_____

Hye Sung Park

Abstract

Solar cells, which have been attracting attention as environmentally friendly and safe candidate as a next generation energy sources, have been studied and used in active layer materials of various structures and materials, from silicon-based crystal structures to organic-based amorphous structures. However, research to find a new active layer to overcome the economical limitations, physical and chemical limitations and fabrication cost of materials is still active. Among the accomplishments of this research, the organic-inorganic hybrid perovskite, which achieved 21% efficiency in the recent years, is the most noteworthy material in solar cell research in the last few years. To maximize the perovskite solar cells performance, there are many researches has been made on the electron transport layer, absorbing layer and hole transport layer. Despite of the so much advance in the device performance and the basic understanding of the perovskite crystal structure formation, the influence of various atmosphere gas during processing condition on perovskite crystal structure research is still in progress. Annealing process were used to convert precursor solution into favorable perovskite absorbing layer by changing composition of precursor or temperature. But there is lack of studies on affected by atmosphere condition during annealing process.

In this work, we investigated the influence of annealing perovskite films deposited on the n-type metal oxide, Zn_2SnO_4 nanoparticles in the different atmosphere (i.e. air, oxygen and argon). While annealing the perovskite, there were no substantial variation in optical properties of perovskite itself. But in argon atmosphere, using Zn_2SnO_4 as an electron transport material, photovoltaic parameter dramatically decreased than oxygen and ambient condition. We found that exposure to argon atmosphere during thermal annealing of the perovskite layer, the interface of zso/perovskite changes in argon atmosphere condition. Using Zn_2SnO_4 as an electron transporting material, built in potential of each various gas condition was different. In argon condition its V_{bi} was much lower than ambient and oxygen condition annealed. Because of the low V_{bi} than other gas condition, we believe that depletion layer was shorter than other gas condition, revealing lower open circuit voltage and fill factor. Also, we found that exposure to argon atmosphere during thermal annealing of the perovskite layer, amount of lead iodide was different in each gas condition detected by GIWAXS images. In order of Ambient<Oxygen<Argon the lead iodide was confirmed. We believe that proper amount of PbI_2 species in the GBs possibly reduce the recombination in the GBs and zso/perovskite surface resulting high device performance. We found that exposure to argon atmosphere during thermal annealing of the perovskite layer, interface Zn_2SnO_4/Perovskite correlates strongly with photophysical properties of the perovskite and affect the device performance. The best performance of perovskite device revealed in ambient condition (25 ℃, 25 % humidity) using Zn_2SnO_4 electron transporting material with power conversion efficiency of 22.35 % in small cells.

List of figures

.

List of tables

Contents

I. Introduction

1.1 The emergence of perovskite solar cells

If Solar cells with an efficiency of 15% can be installed on 0.4% of the Earth's surface, it could provide the total energy needed on Earth at present. Semiconductor-based solar cells, which are widely used today, have the necessary efficiency, but they have not achieved comparative advantage over fossil fuels in terms of production costs and scarcity of materials. Therefore, the current direction of solar cell research is to find materials with high efficiency and to develop low-cost fabrication technology. Commercialized semiconductor-based solar cells require a long time to recover opportunity cost due to high cost or manufacturing cost. This cost problem has led to the need for low-cost solar cell research, the possibility of dye-sensitized solar cells, organic solar cells, and the recent discovery and research of low-cost solar cells, including perovskite solar cells has been emerged. These low cost solar cells have various application possibilities due to their low production cost, thin thickness, light weight, and unique elasticity, but low efficiency and short life span remain critical issues to be solved yet. Over the past two decades, the efficiency of DSSC and OPV has reached 10% to 13% in controlled laboratory environments. PPV, on the other hand, did not take five years to achieve 20% efficiency in a controlled laboratory environment. Due to the high open circuit voltage and the relatively wide energy band gap, it is possible to achieve a tandem solar cell structure with a semiconductor-based solar cell achieving the two purposes of low cost and high efficiency. Researches in perovskite materials has a long history since its discovery in 1839 but applying the materials for photovoltaic usage is happened very recent. It is widely recognized that the first peer-reviewed perovskite solar cell paper was produced by Tsutomu Miyasaka, an electrochemist from Toin University of Yokohama in Japan, and his co-workers in 2009[1]. They treated a film of TiO_2 with a solution containing CH_3NH_3I and PbI_2 and obtained a conversion efficiency of 3.8% for $CH_3NH_3PbI_3/TiO_2$ where J_{sc} = 11.0 mA/cm^2, V_{oc} = 0.61 V and FF = 0.57. After that, a lot of perovskite solar cell researches has been carried out all over the world, especially in Japan, South Korea, England, Switzerland, China, Spain and U.S. And recently perovskite solar efficiency went up to more than 21 %. Many techniques made perovskite solar cell could go up 3% to 21% efficiency. Solvent engineering[2], PbI_2 excess[3], searching for proper electrode for perovskite solar cell.

1.2 Motivation and Aim of research

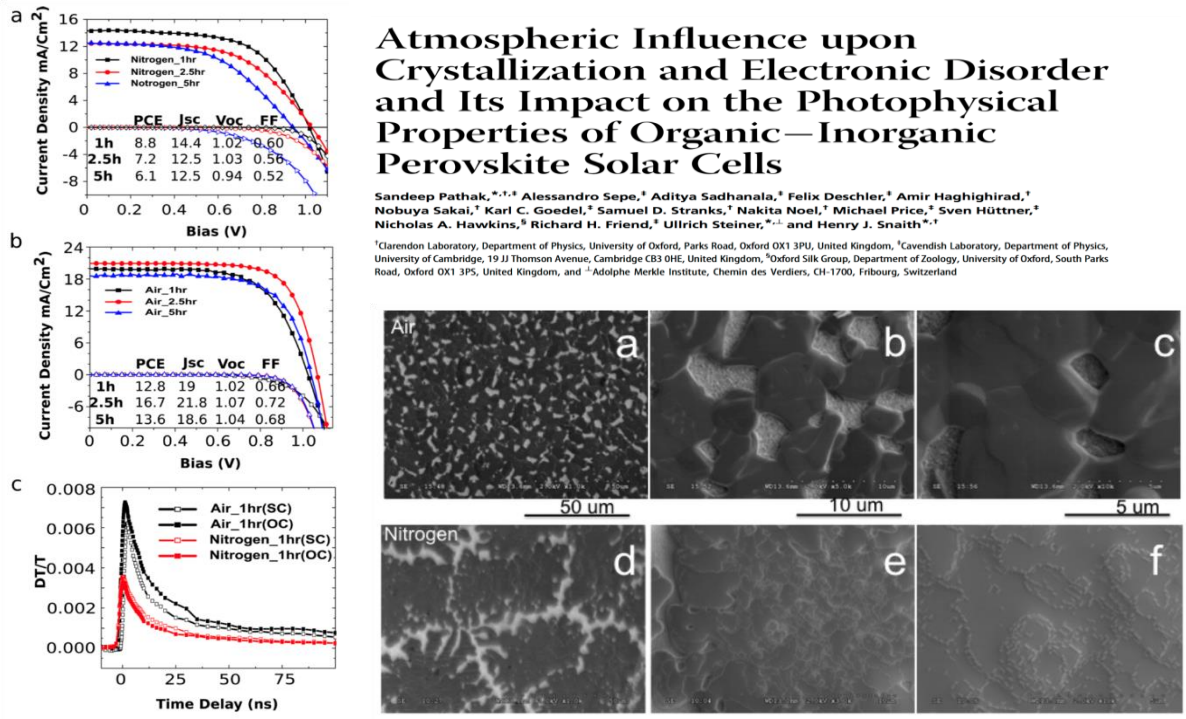

Figure 1. Atmosphere influence during annealing the $MAPbI_3$ in air and nitrogen[4]

Despite so much advance in the device performance and the basic understanding of the perovskite crystal structure formation, the influence of various atmosphere gas during process condition on perovskite crystal structure research is still in progress. Annealing process were used to convert precursor solution into favorable perovskite absorbing layer but there was lack of studies on affected by atmosphere condition during annealing process. Therefore, it looks clear that during annealing process, atmosphere condition that surrounding the perovskite is critical point make fine perovskite solar cells. But, there are still debates about does oxygen really improves the perovskite solar cells and nitrogen or argon cause the defect on the perovskite. As a result, I experimented with $FaPbI_3$ to observe the overall phenomena of how the atmosphere effects on the perovskite solar cells.

Perovskite solar cells (PSCs) and Zn_2SnO_4

2.1 Perovskite light absorbing material

The organic-inorganic halide perovskites can be represented by the chemical formula ABX_3, where the A is the organic cation, B is divalent metal cation (e.g. Cu^{2+}, Ni^{2+}, Co^{2+}, Fe^{2+}, Mn^{2+}, Cr^{2+}, Pd^{2+}, Cd^{2+}, Ge^{2+}, Sn^{2+}, Pb^{2+}) and X is the halide anion (e.g. I^-, Br^- and Cl^-). In ideal cubic unit cell, the component A sites at the center of cubic, and BX_6 octahedral share corners of cubic with a three-dimensional network connection.

The most widely known organic-inorganic hybrid metal halide perovskite is an ABX_3 as structure with methylammonium (MA: CH_3NH_3) or formamidinium (FA: H_2NCHNH_2) as its cation in **figure 1 Zn_2SnO_4 in PSCs**. Such a hybrid perovskite structure has advantages of high efficiency, long photoluminescence lifetime, high carrier mobility and long carrier diffusion length. Furthermore, the ban gap engineering allowed by introducing of mixed halide. The band energy levels of MAPbI3 has direct bandgap of 1.55eV, low excitation binding energy, and high absorption coefficient. Also, bandgap of MAPbI3 corresponds to an absorption onset of 800 nm as well as their high absorption coefficient is higher than the organic dyes, leading to more light can absorb in solar cells.

2.2 Working principle

The basic operating principles of solar cells are illustrated in **figure 4**. The working mechanism is divided by 3 main steps: (1) light absorption of perovskite for generating electrons, (2) electron and hole injection from perovskite to ETM and HTM (Charge separation), respectively and (3) electron and hole transport to each electrode through ETM and HTM network (Charge collection). In addition, the overall energy conversion efficiency (η) of solar cells is determined by open circuit voltage (V_{oc}), short circuit density (J_{sc}), and fill factor (FF), and the intensity of the incident light (I_s).

2.3 Device structures of PSCs

Currently studied perovskite solar cell has two types of structure. The first is a structure in which porous TiO_2 nanoparticles are used as an electron acceptor and a thin compact TiO_2 layer contact is sandwiched between the active layer and a fluorine doped tin oxide substrate. As **figure 3.a and c** the excited electrons reach the contact point at a short distance. The second is a planar heterojunction structure, which requires a long distance between electrons and holes (see **figure 3.b and d**) but is widely used because of the sufficient charge diffusion length of the hybrid and perovskite. These two different structures show similar efficiency and performance

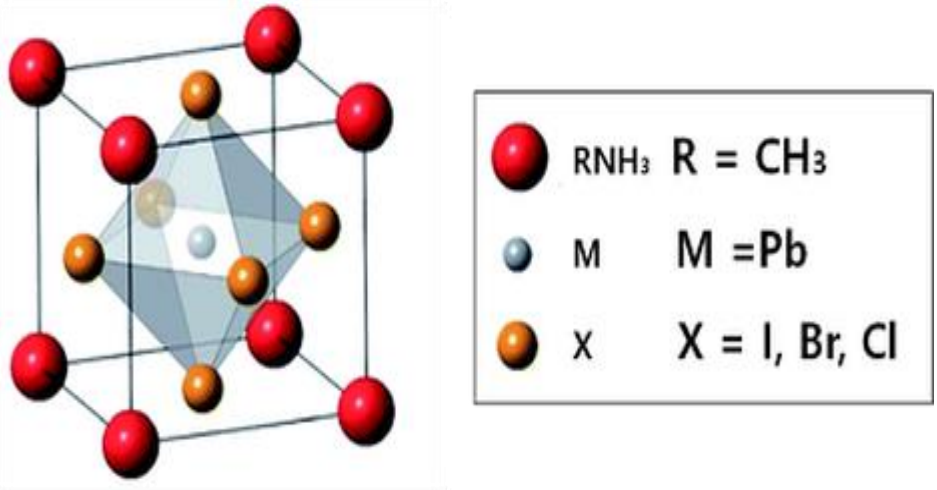

Figure 1. Crystal structure of the perovskite material.

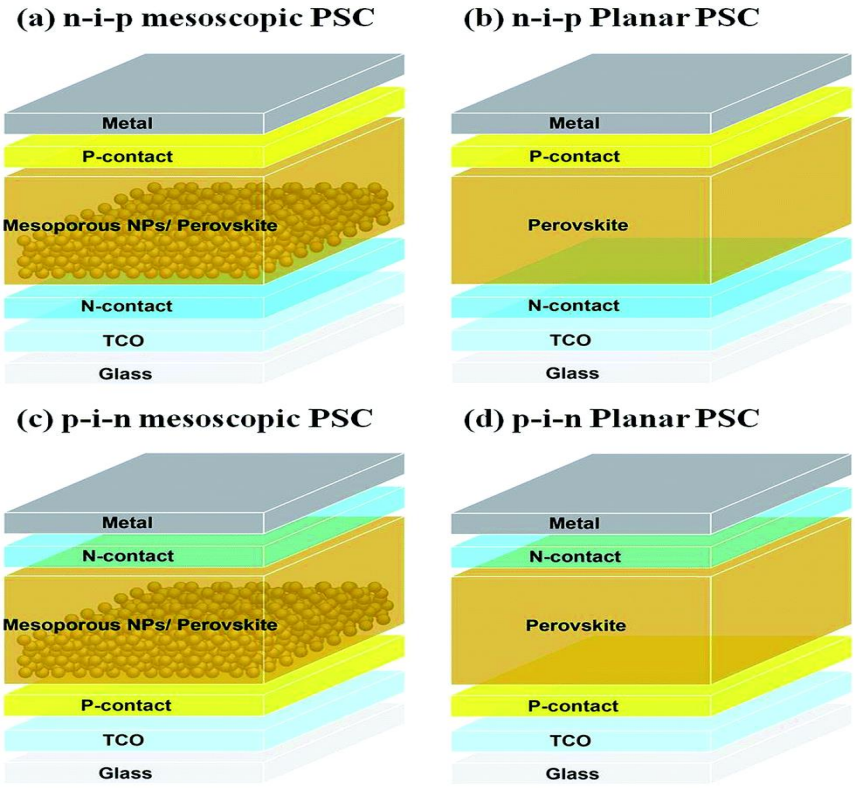

Figure 2. Typical structure of perovskite solar cells[5] (a-d)

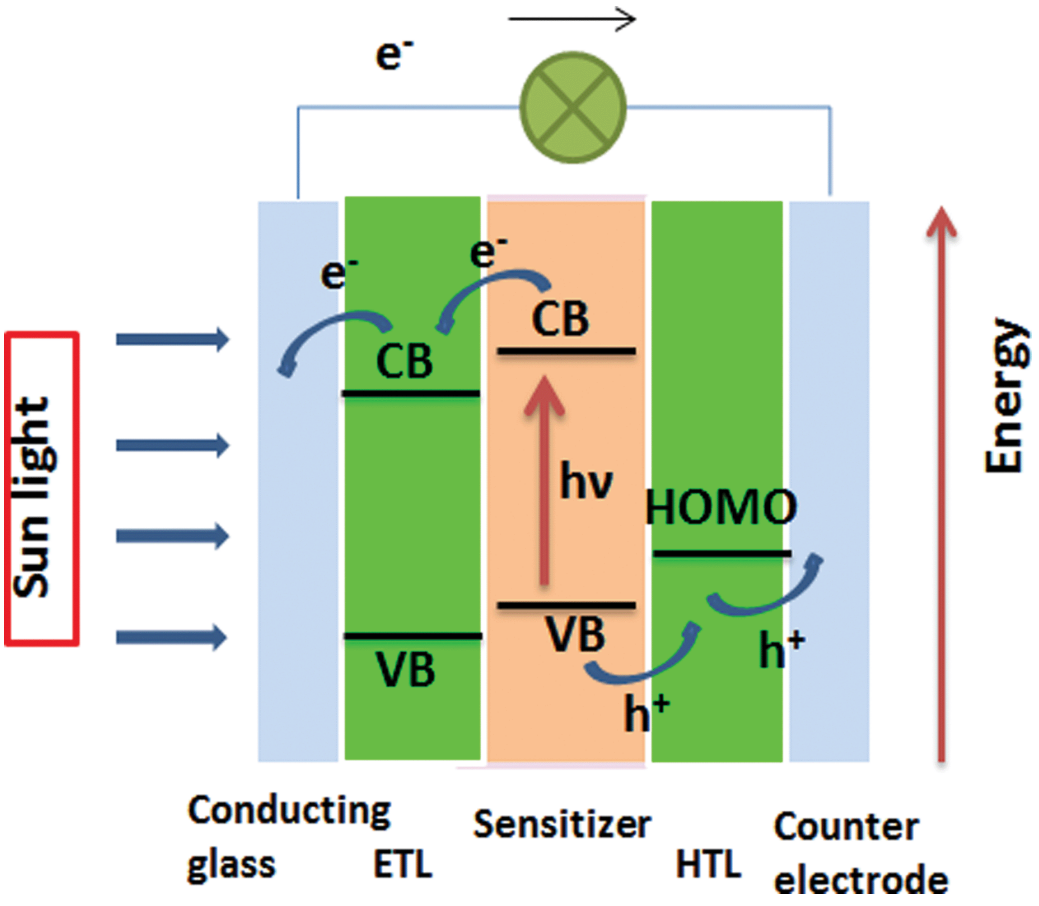

Figure 4. Schematic illustration of the basic operation principle of perovskite solar cell.[6]

2.4 Zn_2SnO_4 in PSCs

Materials of electron transport layer can receive electronic carriers and can effectively transfer them. N-type semiconductor is usually used in electron transport materials, which can make the free electron concentration greater than hole concentration. Compared with perovskite materials, in order to receive the transfer electron into FTO from absorb layer, the conduction band should have smaller minimum value and electron transport layer should have higher electron mobility. In the sequential structure of planar heterojunction perovskite solar cells, the quality of interface, electron transport layer/perovskite layer, affects the device photovoltaic performance. The result is that the energy level matching is advantageous to generate higher open-circuit photovoltage in perovskite solar cell[7].

Research about inorganic materials for electron transport layer has widely conducted including TiO_2[8,9,10], ZnO[11,12], SnO_2[13], Nb_2O_5[14], and In_2O_3[15]. In compare of binary oxides, multi cation oxides have more freedom to tune the materials chemical and physical properties by altering the compositions. Considering the availability of a wide range of multi cation oxides and their tunable properties, it is interesting to investigate their application in perovskite solar cells. In this paper, we used Zn_2SnO_4 nanoparticles in perovskite solar cell. Zn_2SnO_4 is representative ternary tin-based oxide. It is n-type oxide semiconductor and it exists as a cubic inverse spinel structure as showed in **figure 6**. It has small electron effective mass of 0.23 m_e and high electron Hall mobility[16] 10-30 cm^2Vs^{-1}. Also, it has as wide band gap more than 3.5 eV and relatively low refractive index of ~0.2 in the visible spectrum[17].

Generally, Zn_2SnO_4 is synthesized by hydrothermal rout with a strong base, such as NaOH, via intermediate phase $ZnSn(OH)_6$. However, the defect of this method is that strong base can lead aggregation and rapid growth of the intermediate phase of ZSO resulting big size of nanoparticle that cannot use in PSC. Therefore, it is essential to control intermediate phase for synthesizing well dispersed nano size particle. We used hydrazine to make well dispersed size controlled Zn_2SnO_4

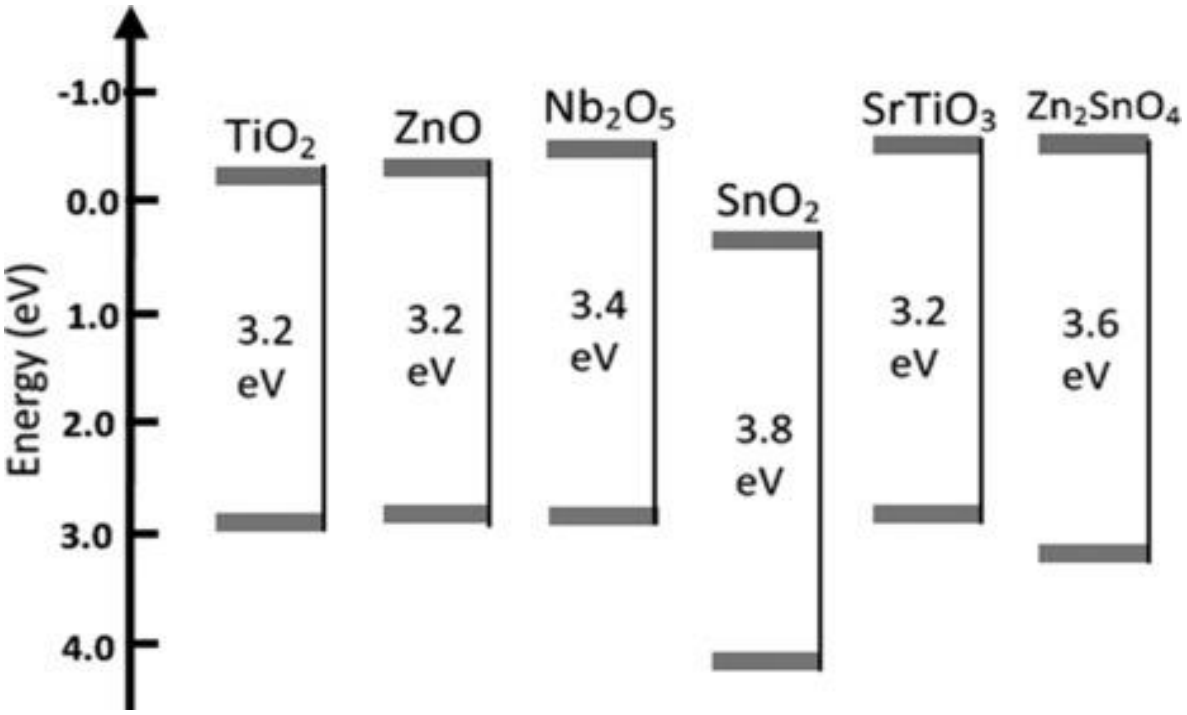

Figure 5. Energy band diagram of Zn_2SnO_4 with other metal oxide materials electron transport layers[18].

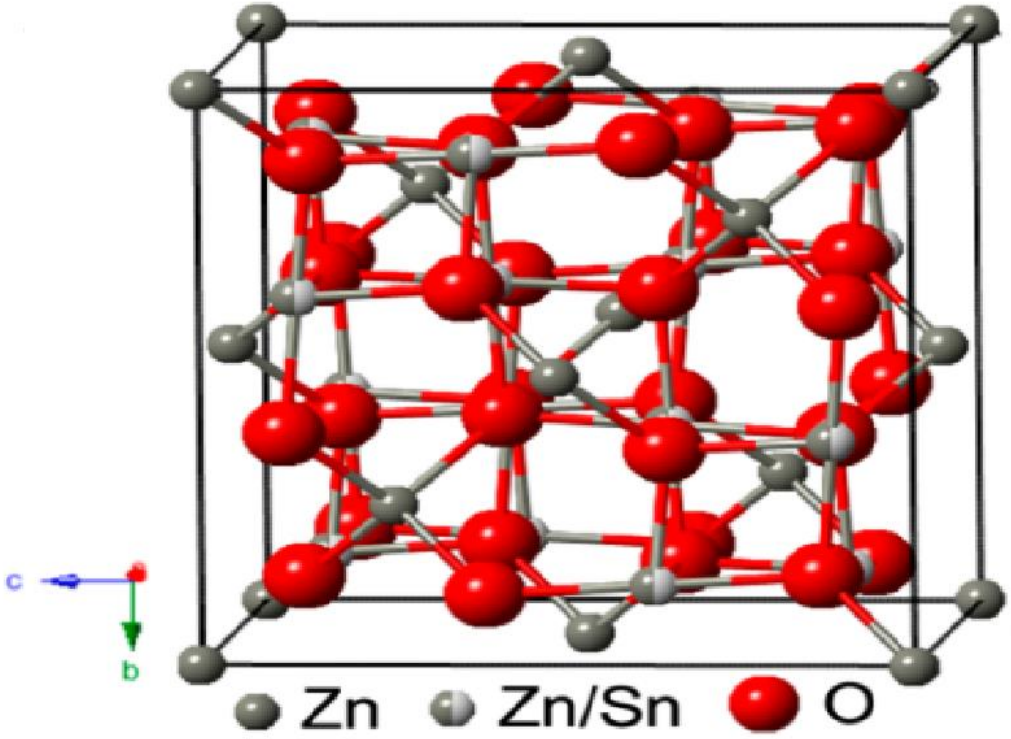

Figure 6. Schematic illustration of inverse spinel structured of Zn_2SnO_4[19].

III. Experimental Method

3.1 Preparation of Zn_2SnO_4 nanoparticles

Preparation of FTO/TiO_2-BL: Patterned fluorine-doped tin oxide (FTO) glasses (Pilkington, TEC8, 8 Ω/cm^2) were ultrasonically cleaned by ethanol for 30 min. Then 20 mM titanium diisopropoxide bis(acetylacetonate) (Aldrich) solution was deposited by spray pyrolysis onto the substrates at 450°C to form a 10 nm-thick TiO_2 BL

Synthesis of Zn_2SnO_4: Zn_2SnO_4 nanoparticles were synthesized by hydrothermal route from the literature. In a typical synthesis, 12.8 mmol $ZnCl_2$ and 6.4 mmol $SnCl{\cdot}5H_2O$ were dissolved in 160 ml of deionized water. Then $N_2H_4{\cdot}H_2O$ (N_2H_4 molar ratio/Zn = 8:1) was slowly added to solution. White precipitates form quickly and move the Teflon-lined autoclave and kept 180°C 12 hr. Zn_2SnO_4 precipitate was then collected and washed with deionized water and ethanol for several times. Finally, Zn_2SnO_4 nanoparticles were dispersed in 2-methoxy ethanol.

3.2 Preparation of $(FAPbI_3)_{1-x}(MAPbBr_3)_x$ films and solar cell fabrication

Solar cell fabrication: Zn_2SnO_4 nanoparticles were deposited onto TiO_2-Bl/FTO substrate by spin-coating method at 3000 rpm for 30 s, following 150 °C hot plate drying. Repeat this procedure 4 ~ 6 times to control thickness of Zn_2SnO_4 electron transport layer. Perovskite layer was fabricated by two-step method. 1.3 M PbI_2-DMSO complex solution in N,N-Dimethylformamide (DMF) were prepared at 80°C. PbI_2 solution then were spin-coated on Zn_2SnO_4 layer at 3000 rpm 30 s and subsequently 465 mM FAI and MABr solution in 2-propanol was spin-coated on top of the PbI_2-DMSO film at 5000 rpm 30 s. Then we anneal at 100 °C 3 hours in each atmospheric condition (air, oxygen and argon). Each fixed the gas flow rates to 10 ppm and to control temperature accurately, we used surface temperature prob (Fluke-62MAX surface thermometer). A set temperature of 100 °C correspond to 96 °C at the hotplate surface. A polytriarylamine (PTAA) were dissolved in toluene 10mg/1ml and spin-coated for 3000 rpm 30 s. Finally, Au counter electrode was deposited by thermal evaporation. The active area of these electrodes was fixed to 16 mm^2

3.3 Characterizations

The absorption spectra were measured using a UV-Vis spectrometer (Jasco V-780). The structure and composition were characterized by XRD (Rigaku D/Max 2500V X-ray diffractometer). The morphology was characterized by FESEM (Hitachi SU-8220) observations. A solar simulator (Newport, Oriel Class A, 91195A) with a source meter (Keithley 2400) at 100 mA cm^{-2} illumination AM 1.5 G and a calibrated Si-reference cell certificated by NREL were used to measure the J-V curves. The IPCE spectra were measured using an internal quantum efficiency system (Oriel, IQE 200B).

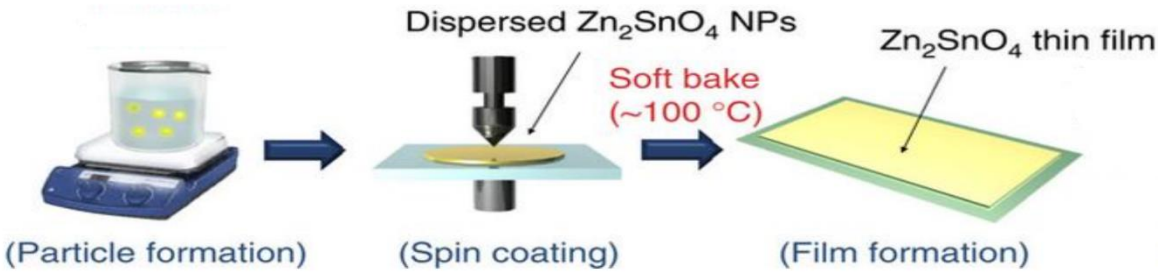

Figure 7. Schematic illustration of synthesizing ZSO and ZSO thin film

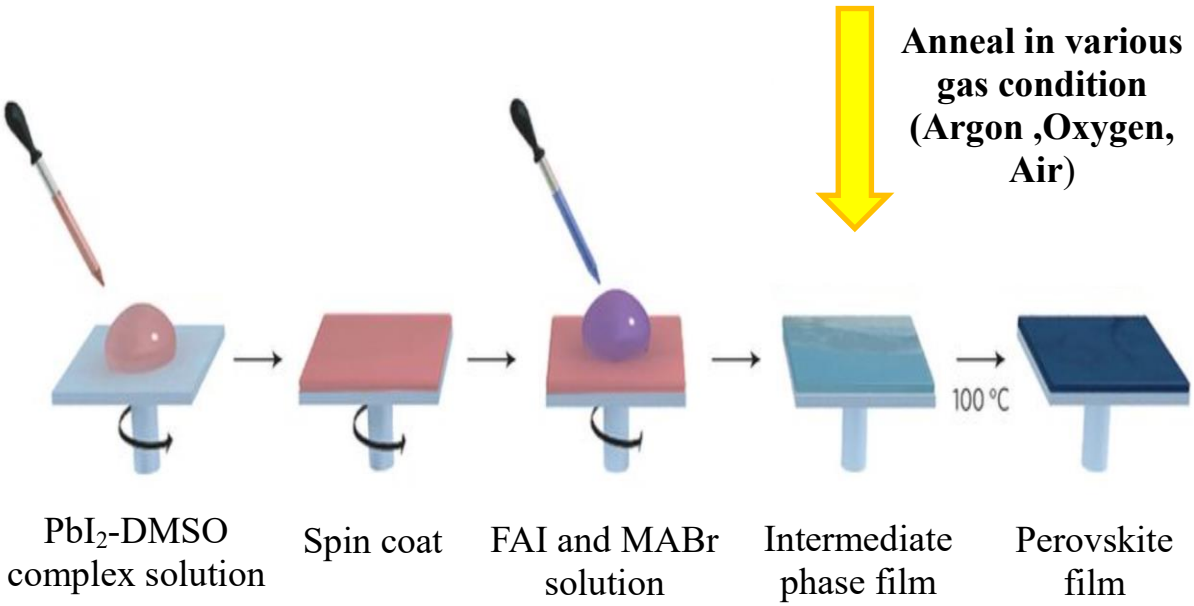

Figure 8. Schematic illustration of making perovskite solar cell which annealed in different atmosphere condition

IV. Results and Discussion

4.1 Zn_2SnO_4 thin film

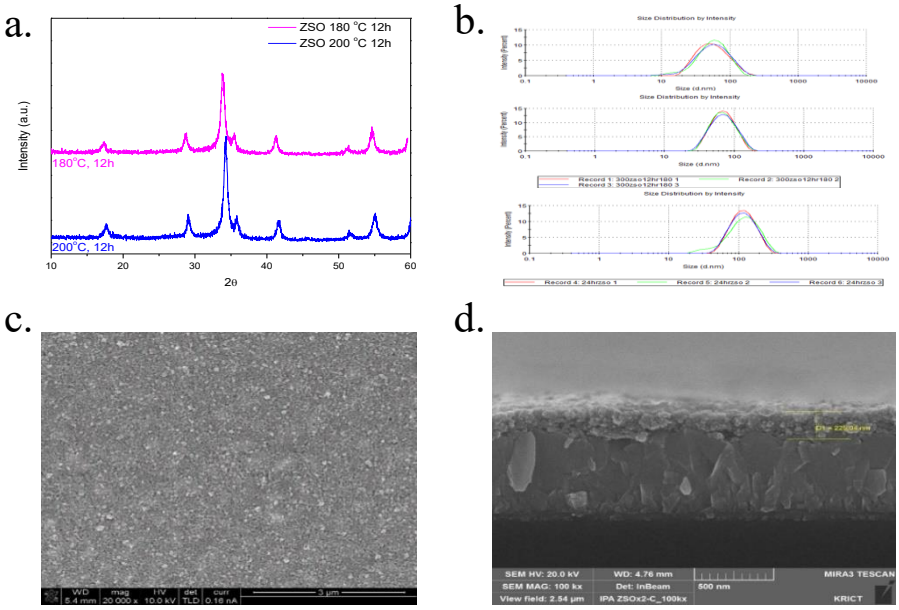

Figure 9. a. X-ray diffraction patterns of the Zn_2SnO_4 NPs. **b**. Z-sizer to check Zn_2SnO_4 nanoparticle size. **c,d**. Scanning electron microscopy(SEM) surface images of Zn_2SnO_4 NPs surface image and cross image.

Sample	**TiO_2**	**Zn_2SnO_4**
Band gap (eV)	~3.0	>3.6
Mobility [$cm^2/V{\cdot}S$]	0.1~4	15~30
Transmittance	Bad	Good
Photo-stability	Bad	Good
Chemical-stability	Good	Good

Table 1. The properties of Zn_2SnO_4 compared to TiO_2.

We used ZnSnO4 nanoparticle as a n-type electrode layer, because their mobility, transmittance, and chemical stability are more better than TiO_2 nanoparticles. In figure, we have successfully synthesized the ZSO nanoparticles. The nanoparticle size was 25 nm ~ 60 nm. ZSO thickness were fixed to 120nm ~ 150 nm because of the optimized thickness for high performance perovskite solar cells. Surface image shows that the coverage of ZSO on the FTO glass substrate. It is clear that ZSO nanoparticles were well dispersed and they were able to cover the surface of the substrate.

4.2 Atmospheric dependence on the efficiency of perovskite solar cells

The precursor solution used here to deposit perovskite film is $(FAPbI_3)_{0.85}(MAPbBr_3)_{0.15}$ that provides better performance than methylammonium lead iodide because of its broad absorption spectrum, low hysteresis[20] and their thermal stability[21]. For electron transporting material, planar structure Zn_2SnO_4 nanoparticles were deposited on the fluorine-doped tin oxide(FTO)-coated glass substrate, coated with an n-type TiO_2 compact layer. During the process of fabricating perovskite layer, the samples were annealed isothermally at 100 ℃ 3 hours (optimized perovskite annealing time, **figure 12,13 and table 4**) at different atmospheres as a nitrogen, oxygen and ambient condition (temperature 25 ℃, humidity 25 %) and fixed the perovskite deposition methodology as a two-step sequential to neglect the all possibilities that can affect the device performance. Subsequently, poly(triaryl amine) was deposited as a p-type hole transporting layer. **Figure 10.** shows the representative J-V curves for ambient, oxygen, argon condition PSCs. The photovoltaic parameters are summarized in **table 2**. Using Zn_2SnO_4 nanoparticles as electron transporting material, ambient and oxygen condition showed similar device performance. But in argon atmosphere, each photovoltaic parameter reduced, especially open circuit voltage and fill factor causing low device efficiency. We thought if the argon condition annealed devices are additionally annealed in ambient condition, photovoltaic parameters could optimize itself. Nevertheless, photovoltaic parameters did not reveal optimizing effect itself but revealing similar tendency of only argon atmosphere condition annealing method in 3 hours (**figure 11. and table 4**). However, annealing the absorbing layer in the ambient condition and additionally annealed in the argon gas condition, device performance was steady as annealed in air condition. Depositing the same perovskite and p-type material, we only could suspect that perovskite and Zn_2SnO_4 NPs/perovskite interface could affected by atmosphere condition during annealing causing low efficiency.

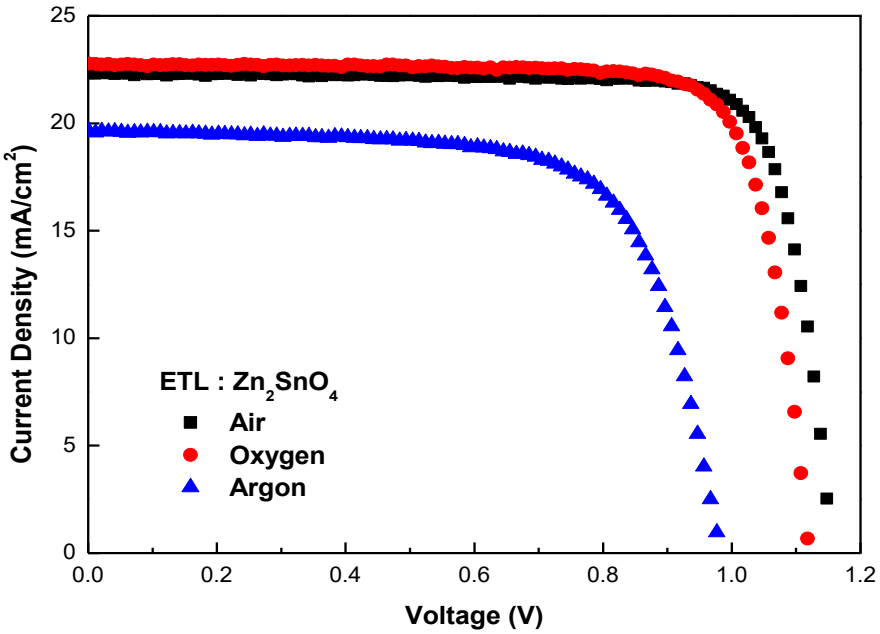

Figure 10. Current density -voltage characteristics. perovskite solar cell device performance using Zn_2SnO_4 NPs at each different atmospheric condition

Zn_2SnO_4 NPs	Jsc (mA/cm2)	Voc (V)	FF (%)	Efficiency (%)
Air	22.32	1.16	81.4	21.04
Oxygen	22.78	1.12	80.32	20.45
Argon	19.64	0.99	69.65	13.50

Table 2. Photovoltaic parameters of each figure 7.

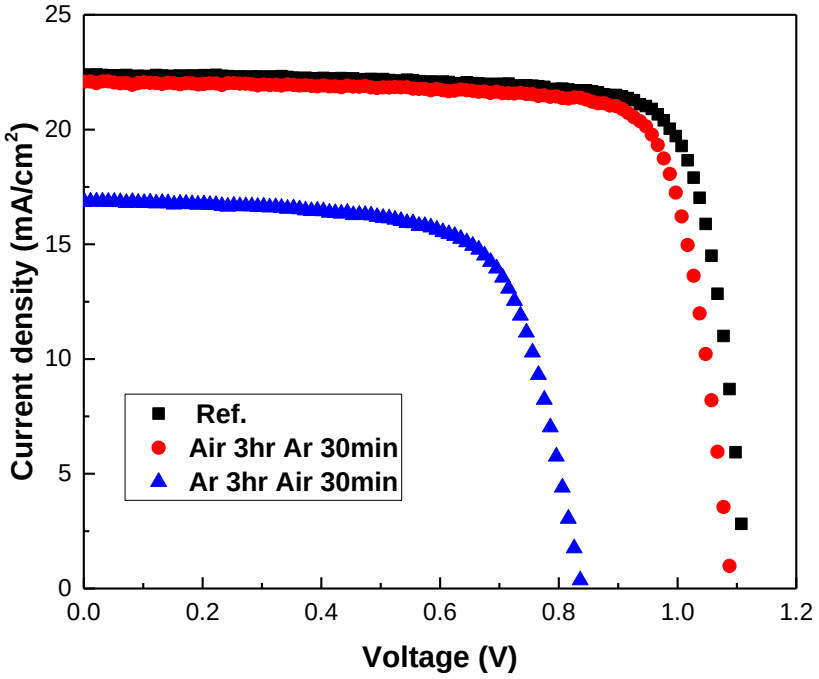

Figure 11. Current density-voltage characteristics of two atmospheric condition annealing to see perovskite self-heal in the ambient condition

	J_{sc}(mA/cm2)	V_{oc} (V)	FF (%)	Efficiency (%)
Air condition(Ref.)	22.39	1.12	79.88	19.99
Air 3 hours, Argon 30 min	22.09	1.09	79.41	19.08
Argon 3 hours, Air 30 min	16.85	0.84	69.74	9.82

Table 3. Photovoltaic parameters of figure. Perovskite solar cell device. After argon atmosphere anneal, we additionally annealed the device in the ambient condition.

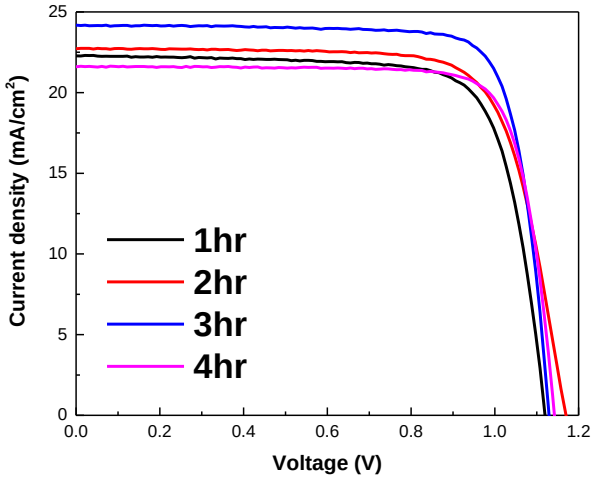

Figure 12. Current density-voltage characteristics of annealing time of perovskite solar cell in ambient condition

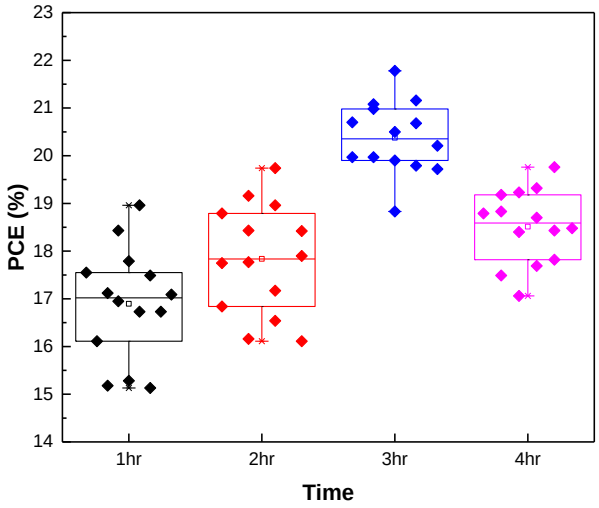

Figure 13. Histogram of the ambient condition annealing device PCE distribution

	J_{sc}(mA/cm^2)	V_{oc} (V)	FF (%)	PCE (%)
1 hour	22.3	1.12	76.2	18.96
2 hours	22.7	1.17	74.4	19.74
3 hours	23.6	1.15	80.8	21.78
4 hours	21.6	1.14	80.38	19.76

Table 4. Photovoltaic parameters of figure. Perovskite solar cell device.

Before investigating interface between Zn_2SnO_4 NPs and absorbing layer, we wanted to confirm that absorbing layer properties that annealed in each argon, oxygen and ambient condition. Atmosphere defended XRD patterns of the as prepared $(FAPbI_3)_{0.85}(MAPbBr_3)_{0.15}$ film on FTO substrate shows typical diffraction pattern of the trigonal perovskite $(FAPbI_3)_{0.85}(MAPbBr_3)_{0.15}$ thin film, see **Figure 14.** According to XRD results, during thermal annealing process, ambient, oxygen and argon atmosphere condition didn't affect the perovskite phase changing. X-ray diffractograms of each different atmospheric annealed sample showed same degree of preferred orientation and lead halide peaks for all samples. For further observation of perovskite optical properties and morphology, absorption spectroscopy experiment and scanning electron microscopy (SEM) were performed on air, oxygen, and argon atmosphere. In absorption spectrum. **Figure 15.** shows the UV-absorption spectra of annealed the perovskite absorbing layer in each different atmosphere condition. All samples of perovskite layer were annealed for 3 hours in ambient, oxygen, and argon condition. Bandgap of $(FAPbI_3)_{0.85}(MAPbBr_3)_{0.15}$ was almost 1.54 eV, near the same values of reported $FAPbI_3$ bandgap 1.55eV. Scanning electron microscopy (SEM) images of the perovskite surface layer were show in **figure 16**. It is surface images that annealed the perovskite layer in each different gas condition (e.g. Argon, Oxygen, and air). There was no distinguishable difference in morphology and bandgap in air, oxygen, and argon condition. It's indicating that annealing the different atmosphere condition does not relate to formation of perovskite morphology. However, device performance was significantly different when perovskite layer was annealed in argon atmosphere condition using Zn_2SnO_4 as an electron transporting material.

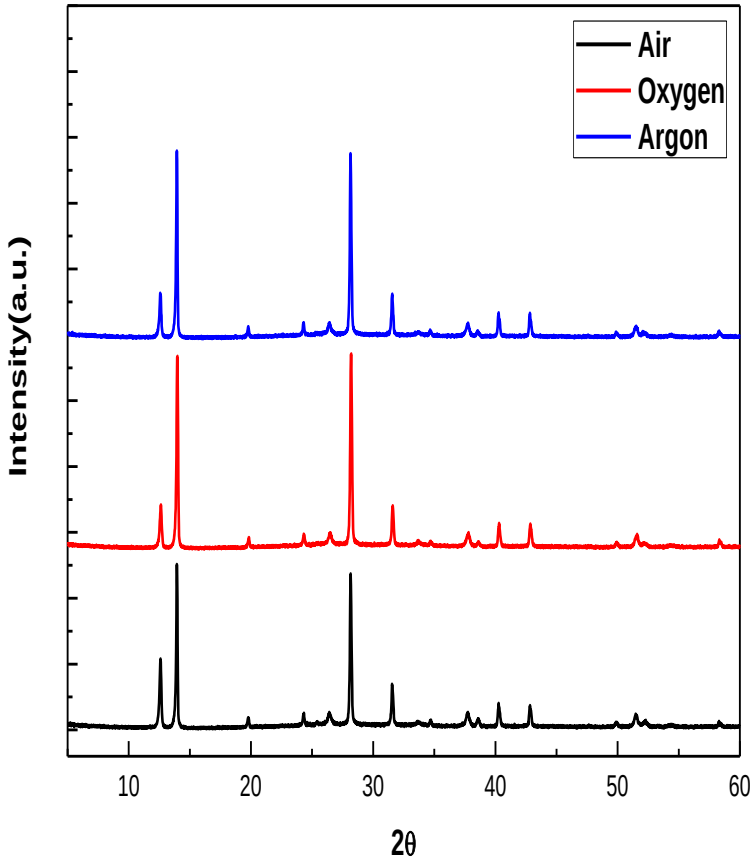

Figure 14. X-ray diffraction patterns of the air, oxygen, and argon atmosphere annealed in 100 ℃ 3 hours.

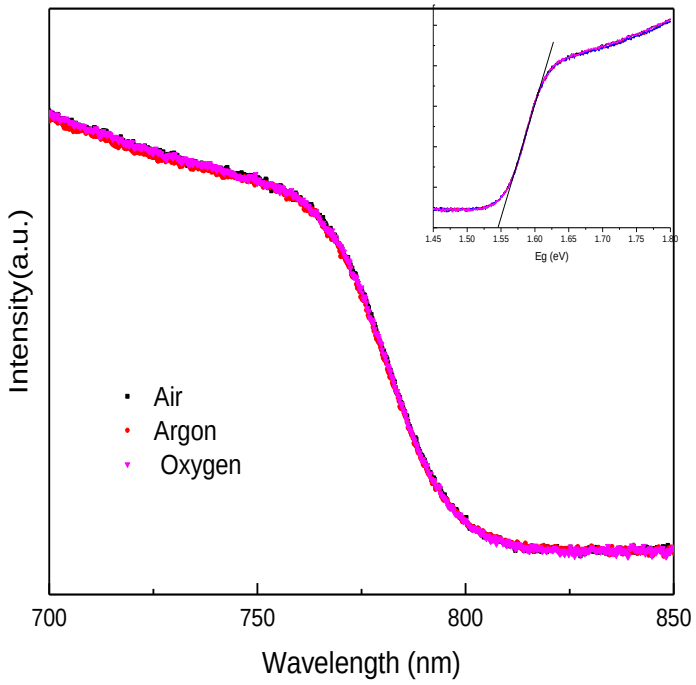

Figure 15. UV-absorption and band gap of annealing perovskite in air, argon, and oxygen condition

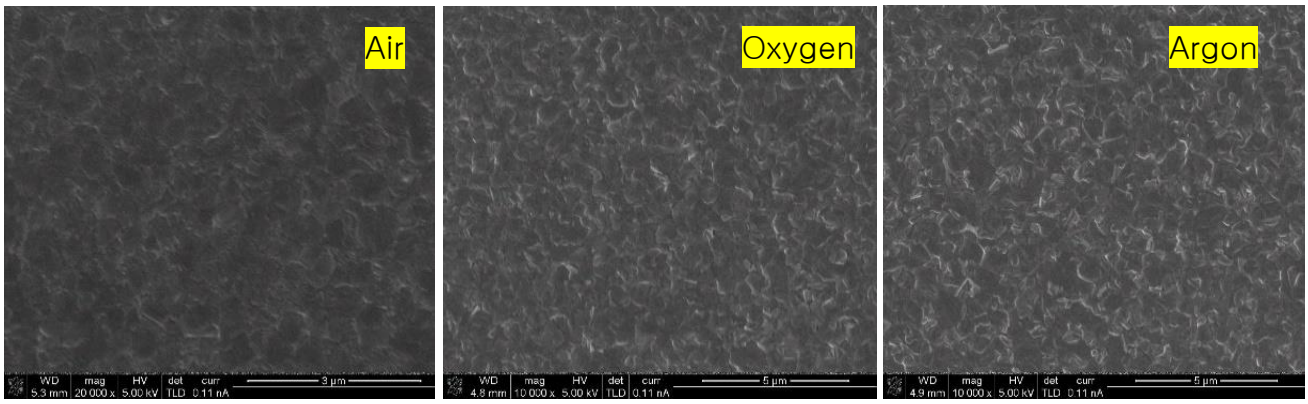

Figure 16. Scanning electron microscopy(SEM) surface images of perovskite layers spin coated in air, oxygen, and argon.

To further understand about decrease of current density of perovskite solar cell, EQE performed in each different atmosphere condition annealed devices. Perovskite annealed in argon condition, the current density was lower than oxygen or ambient condition as shown in **figure 17**.

To investigate the effect of atmosphere condition during annealing the perovskite absorbing layer on fill factor and open circuit voltage, impedance spectroscopy (IS) analysis was performed under dark giving bias voltage of 0.9 V. **Figure 18. a** presents the Nyquist plots of each atmosphere condition annealed perovskite solar cells. Measuring each different gas annealed samples in the dark, the semicircle in the high frequency region results from the selective contact or interfaces of this contact which contributes to series resistance(R_s) and the recombination process can be observe in the low frequency region[22]. Measuring in the dark condition and having same device structure, Nyquist plot in the low frequency region, there were distinguishable results by annealing the perovskite absorbing layer in each gas condition. The recombination resistance increased following the series Argon < Oxygen < Air. This result could relate to open circuit voltage increasing following the order of Argon < Oxygen < Air. Because of the hole transport layer, absorbing layer and electron transport layer were identical, we assumed that during the annealing process, argon atmosphere could affect the interface zso/perovskite. To understand the junction between absorbing layer and Zn_2SnO_4 NPs, Mott-Schottky (MS) measurement for ZSO/perovskite were conducted[23](**Figure 18. b**). Measurement of MS was conducted in the dark situation and gave 0.9 bias voltage that was already measured by a solar simulator with a source meter at 100 mA cm^{-2} illumination AM 1.5 G as an output voltage. Using V_{bi}, the depletion width is calculated according to[24]:

$$W_{p,n} = \left\{ \frac{2\varepsilon_s V_{bi}}{e} \left[\frac{N_a + N_d}{N_a N_d} \right] \right\}^{1/2} \qquad (1)$$

In eqn (1), N_a and N_d are the doping densities of the acceptor and the donor, respectively. ε is the static permittivity, e is elementary charge. The permittivity of $(FAPbI_3)_{0.85}(MAPbBr_3)_{0.15}$ was calculated to be 46.9 and Zn_2SnO_4 to be 10. In Mott-Schottky plot, x-axis determines the built-in voltages, which is full cell that only different in atmosphere annealing condition. The thickness of the Zn_2SnO_4 NPs layer was almost fixed to 110 ± 20 nm and perovskite layer 450 ± 10 nm.

Figure 18.b ambient and oxygen condition annealed device built-in voltage was near 0.92 V and argon condition annealed built-in voltage was near 0.58 V. The total depletion width (W_t) was calculated in **table 5**.

	Ambient	Oxygen	Argon
Perovskite thickness (nm)	450 ± 20	450 ± 10	450 ± 20
Zn2SnO4 NPs thickness (nm)	130 ± 20	130 ± 20	130 ± 20
V_{bi} (V)	0.92	0.92	0.58
W_n (nm)	32	32	25
W_p (nm)	218	218	173
$W_n + W_p = W_t$ (nm)	250	250	198

Table 5. Calculated depletion width, built-in voltage in different atmosphere annealed PSC.

The observation of depletion layer width, ambient condition and oxygen condition were 250 nm similar values of half of the thickness of the zso/perovskite. However, in argon atmosphere condition annealed device, the depletion layer was shorter than other atmosphere condition resulting low efficiency. It is suggesting that depletion region assists the charge separation and suppress the back reaction. Consequently, during the annealing the perovskite layer above the Zn_2SnO_4 NPs layer, ambient, oxygen and argon condition did not affect the any of perovskite optical properties or morphology itself. However, annealing in the perovskite in argon atmosphere condition affect the properties of interface between absorbing layer and electron transport layer moreover, leading to low power conversion of perovskite devices.

Furthermore, to explain the high performance of the of Zn_2SnO_4/perovskite device, 2D GIWAX was measured in each atmosphere condition. In **figure 19.** is the results of GIWAXS 2D images. It is indicating that PbI_2 remained in order of Air < Oxygen < Argon when tendency according to the type of carrier gas used during the heat treatment was observed. For further confirmation of possibility of the PbI_2 passivation effect[25] on zso/perovskite, scanning electron microscopy (SEM) and X-ray diffraction (XRD) measurement (see **figure 20.**) was conducted. After 2 hours annealing the absorbing perovskite layer, lead halide peak appears in the XRD patterns. Annealing on the 150 ℃ hot plate for more than 1 hours, perovskite was decomposed where perovskite films to form PbI_2 phase. 100 ℃ 4 hours annealing perovskite solar cell performance was decreased because of lead halide could affect as a passivation of perovskite grain boundary but excessive heat treatment could make lead halide as an insulator. Also, we could see in the SEM images that new species showed relatively bright contrast compared to adjacent grains that speculated to be PbI_2 indicating in the corresponding XRD pattern. As a result, to make PbI_2 to roll positive effect to PSCs device, optimized gas condition was ambient condition and annealing time was fixed to 3 hours at 100 ℃.

In summary, we have demonstrated the atmosphere affect during the perovskite annealing on the Zn_2SnO_4 NPs layer. In argon condition annealed device photo parameters were all decreased. Not because of perovskite changing optical properties or morphology itself and change of Zn_2SnO_4 nanoparticles properties but causing problem between zso/perovskite interface. Also, atmosphere condition and annealing time could induce the PbI_2 in the GBs of the perovskite which is one of the important point to produce high performance perovskite solar cells.

As a result, argon atmosphere caused the change of depletion width of zso/perovskite causing low fill factor and V_{oc}. It is still needing to be research more about inorganic electron transport layer and perovskite lattice mismatch, surface energy and structure (i.e. planar, mesoporous) that can cause the interface defect between ETL/Perovskite. However, in this work, atmosphere condition could be one of the critical element to break through high efficiency of perovskite solar cell. the best performance was 22.35 % efficiency in ambient condition anneal at 100 ℃ for 3 hours (25 ℃, 25 % humidity. **figure 21**).

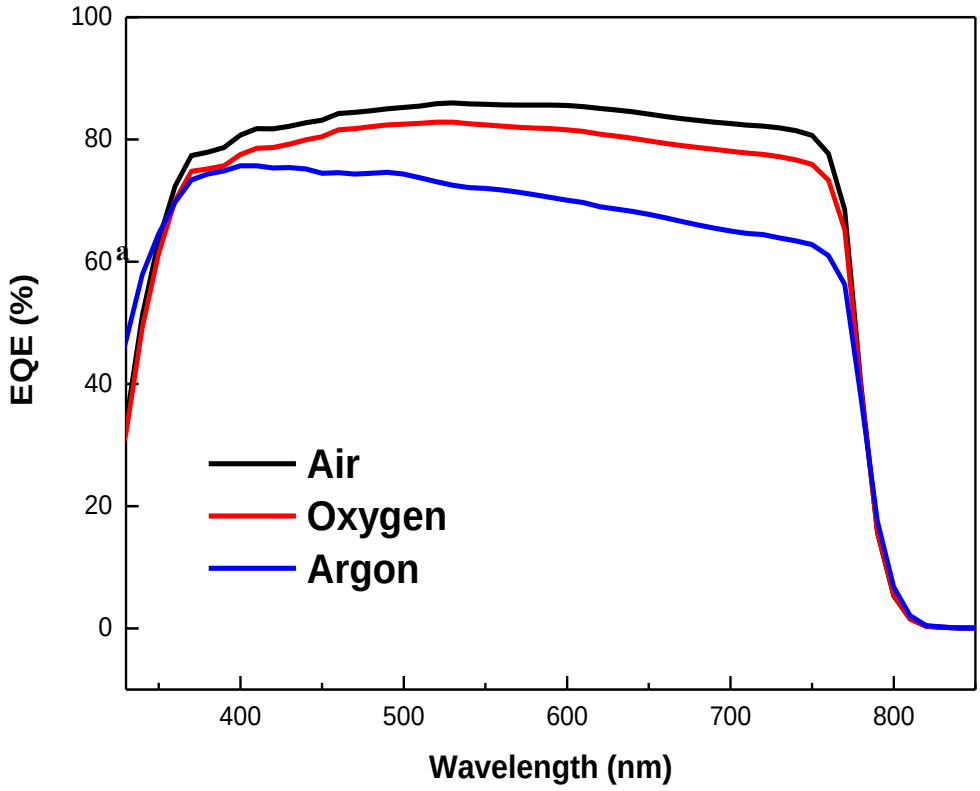

Figure 17. EQE of different atmosphere condition annealed perovskite solar cell device

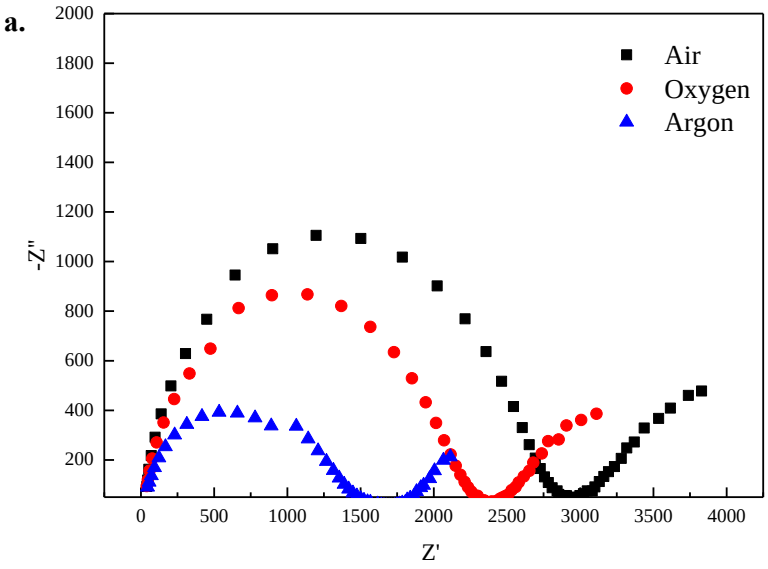

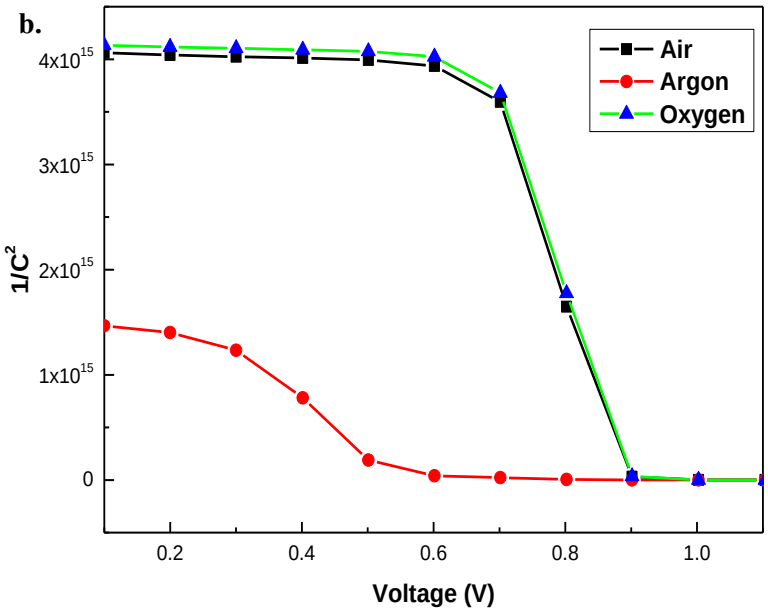

Figure 18. a. Nyquist plots **b.** Mott-Schottky plot

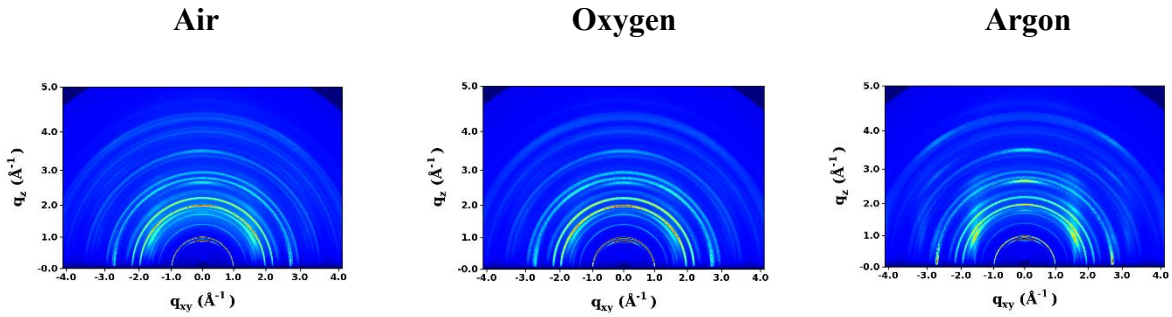

Figure 19. Grazing incidence wide angle x-ray scattering of zso/perovskite annealed in different gas condition

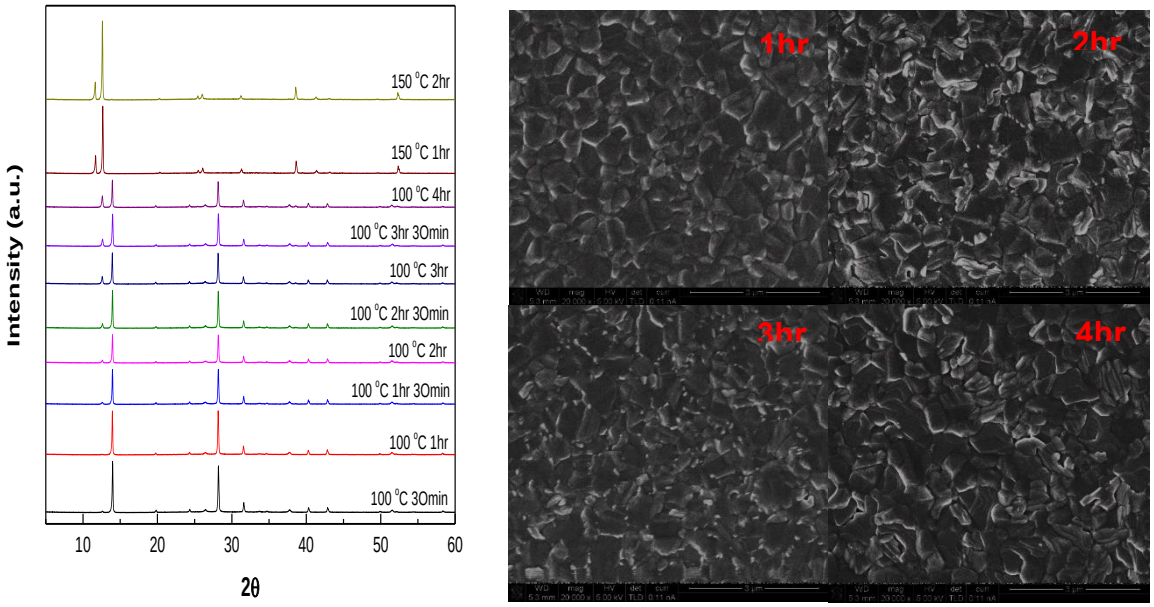

Figure 20. time dependence characterization of the zso/perovskite thin films, by annealing at 100 ℃ in ambient atmosphere.

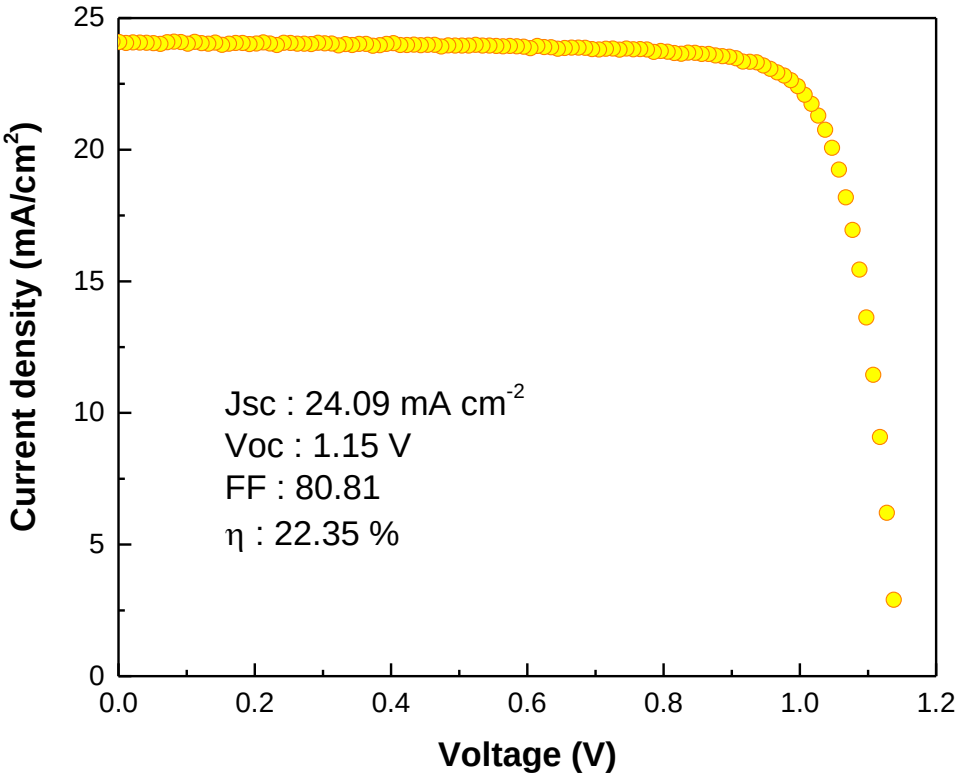

Figure 21.
best performance device. Device structure : FTO/compact-TiO_2/Zn_2SnO_4/$(FAPbI_3)_{0.85}(MAPbBr_3)_{0.15}$ /PTAA/Au. Atmosphere condition : ambient condition

V. Reference

[1] A. Kojima, K. Teshima, Y. Shirai, and T. Miyasaka, "Organometal halide perovskites as visible-light sensitizers for photovoltaic cells.," J. Am. Chem. Soc., 2009, vol. 131, no. 17, pp. 6050–1.

[2] NJ Jeon, JH Noh, YC Kim, WS Yang, S Ryu, SI Seok. Solvent engineering for high performance inorganic organic hybrid perovskite solar cells. Science materials. **2014**, 13 (9), 897.

[3] YC Kim, NJ Jeon, JH Noh, WS Yang, J Seo, JS Yun, SI Seok. Beneficial effects of PbI2 incorporated in organo-lead halide perovskite solar cells. Advanced Energy Materials 2016, 6, 1502104.

[4] Sandeep Pathak, Alessandro Sepe, Aditya Sadhanala, Henry J. Snaith. Atmospheric influence upon crystallizaition and electronic disorder and its impact on the photophysical properties of organic-inorganic perovskite solar cells. ACS Nano, **2015** 9 (3), pp 2311-2320.

[5] Ming-Hsien Li, Jun-Ho Yum, Soo-Jin Moon, Peter Chen. Inorganic p-type semiconductors: Their applications and progress in dye-sensitized solar cells and perovskite solar cells. Energies **2016**, 9, 331, doi:10.3390/en9050331

[6] Zhongmin Zhou, Shuping Pang, Zhihong Liu, Hongxia Xu, Guanglei Cui. Interface engineering for high-performance perovskite solar cells. J. Mater. Chem. A. **2015**, 3, 19205-19217.

[7] Ding XJ, Ni L, Ma SB, Ma YZ, Xiao LX, Chen ZJ. Research progress of electron transport layer in perovskite solar cells. Acta Phys Sin. **2015**;64(3):95.

[8] O'Regan, B.; Graetzel, M. A low-cost, high-efficiency solar cell based on dye-sensitized colloidal TiO2 films. *Nature* **1991**, *353* (24), 737.

[9] Chiba, Y.; Islam, A.; Watanabe, Y.; Komiya, R.; Koide,N.; Han, L. *Jpn. J. Dye-Sensitized solar cells with Converstion Efficiency of 11.1% Appl. Phys. 2* **2006**, *45* (24-28)

[10] Mor, G.K.; Shankar, K.; Paulose, M.; Varghese, O. K.; Grimes, C. A. Use of Highly-Ordered TiO2 Nanotube arrays in dye-sensitized solar cells *Nano. Lett.* **2006**, *6* (2), 215.

[11] Dae-Yong Son, Jeong-Hyeok Im, Hui-Seon Kim, and Nam-Gyu Park. 11% Efficient Perovskite Solar Cell Based on ZnO Nanorods: An Effective Charge Collection System. :J. Phys. Chem. C, **2014**, 118, 30, 16567-16573

[13] Mulmudi Hemant Kumar, Natalia Yantara, Sabba Dharani, Michael Graetzel, Subodh Mhaisalkar, Pablo P. Boix and Nripan Mathews. Flexible, low-temperature, solution processed ZnO-based perovskite solid state solar cells. Chem. Commun., **2013**,49, 11089-11091

[14] Kay, A.; Graetzel, M. Dye-Sensitized Core−Shell Nanocrystals: Improved Efficiency of Mesoporous Tin Oxide Electrodes Coated with a Thin Layer of an Insulating Oxide Chem. Mater. **2002**, 14 (7), 2930

[15] Guo, P.; Aegerter, M. A. RU(II) sensitized Nb2O5 solar cell made by the sol-gel process. Thin solid films. **1999**, *351* (1-2), 290.

[16] Hara, K.; Horiguchi, T.; Kinoshita, T.; Sayama, K.; Sugihara, H.; Arakawa, H. Highly efficient photon to electron conversion with mercurochrome sensitized nanoporous oxide semiconductor solar cells. *Sol. Energy Mater. Sol. Cells* **2000**, *64*, 115.

[17] Coutts, T.J., Young, D.L., Li, X., Mulligan, W. & Wu, X. Search for improved transparent conducting oxides: a fundamental investigation of CdO, Cd2SnO4, and Zn2SnO4. J. Vac. Sci. Technol. A **2000**, 18, 2646-2660.

[18] Young, D.L., Moutinho, H., Yan, Y. & Coutts, T.J. Growth and characterization of radio frequency magnetron sputter-deposited zinc stannate, Zn_2SnO_4, thin films. J. Appl. Phys. **2002**, 92, 310-319.

[19] Shuang Yang, Yu Hou, Jun Xing, Hua Gui Yang. Ultrathin SnO2 Scaffolds for TiO2-Based Heterojunction Photoanodes in Dye-Sensitized solar cells. Chemistry-A European Journal, **2013**. 19(28):p. 9366-9370

[20] Lihong Bao, Jianfeng Zang, Guofeng Wang, Xiaodong Li. Atomic-Scale Imaging of Cation Ordering in Inverse Spinel Zn_2SnO_4 Nanowires. Nano letters, **2014**. 14(11):p. 6505-6509

[21] Nam Joong Jeon, Jun Hong Noh, Woon Seok Yang, Sang Il Seok. Compositional engineering of perovskite materials for high-performance solar cells. Nature. **2015**, 476, Vol 517

[22] Juarez-Perez, E. J.; Wuβler, M.; Fabregat-Santiago, F.; Lakus-Wollny K.; Mora-Sero, I. Roll of the Selective Contacts in the Performance of Lead Halide Perovskite Solar Cells. J. Phys. Chem. Lett. **2014**, 5, 680-685

[23] Brabec, C. J.; Cravino, A.; Meissner, D.; Sariciftci, N. S.; Fromherz, T.; Hummelen, J. C. Origin of the open circuit voltage of plastic solar cells. Adv. Funct. Mater. **2001**, 11, 374−380

[24]. Luther, J. M.; Law, M.; Beard, M. C.; Song, Q.; Reese, M. O.; Ellingson, R. J.; Nozik, A. J. Schottky solar cells based on colloidal nanocrystal films. Nano Lett. **2008**, 8, 3488−3492.

[25] Qi Chen, Huanping Zhou, Tze-Bin Song, Son Luo, Ziruo Hong, Hsin-Sheng Duan, Yang Yang. Controllable Self-induced passivation of Hybrid lead iodide perovskites toward high performance solar cells. Nano Lett. 2014, 14, 4158-4163